Pyrazolo[1,5-*a*]-1,3,5-triazine as a Purine Bioisostere: Access to Potent Cyclin-Dependent Kinase Inhibitor (*R*)-Roscovitine Analogue

Florence Popowycz,[†] Guy Fournet,[†] Cédric Schneider,[†] Karima Bettayeb,[‡] Yoan Ferandin,[‡] Cyrile Lamigeon,[||] Oscar M. Tirado,[§] Silvia Mateo-Lozano,[§] Vicente Notario,[§] Pierre Colas,[‡,||] Philippe Bernard,*[,⊥] Laurent Meijer,*[,‡] and Benoît Joseph*[,†]

Institut de Chimie et Biochimie Moléculaires et Supramoléculaires, UMR-CNRS 5246, Laboratoire de Chimie Organique 1, Université de Lyon, Université Claude Bernard-Lyon 1, Bâtiment Curien, 43 Boulevard du 11 Novembre 1918, F-69622 Villeurbanne, France, CNRS, "Protein Phosphorylation & Human Disease" Group, Station Biologique, B.P. 74, 26682 Roscoff, France, Laboratory of Experimental Carcinogenesis, Lombardi Comprehensive Cancer Center, Georgetown University Medical Center, 3970 Reservoir Road NW, Washington, D.C. 20057-1482, Aptanomics SA, 181-203 Avenue Jean Jaurès, 69007 Lyon, France, Greenpharma SA, 3 Allée du Titane, 45100 Orléans, France

Received October 23, 2008

Pharmacological inhibitors of cyclin-dependent kinases (CDKs) have a wide therapeutic potential. Among the CDK inhibitors currently under clinical trials, the 2,6,9-trisubstituted purine (*R*)-roscovitine displays rather high selectivity, low toxicity, and promising antitumor activity. In an effort to improve this structure, we synthesized several bioisosteres of roscovitine. Surprisingly, one of them, pyrazolo[1,5-*a*]-1,3,5-triazine **7a** (N-&-N1, GP0210), displayed significantly higher potency, compared to (*R*)-roscovitine and imidazo[2,1-*f*]-1,2,4-triazine **13** (N-&-N2, GP0212), at inhibiting various CDKs and at inducing cell death in a wide variety of human tumor cell lines. This approach may thus provide second generation analogues with enhanced biomedical potential.

Introduction

Pharmacological inhibition of cyclin-dependent kinases (CDKs) is anticipated to provide an effective approach to the control of multiple human diseases in the clinic including cancers, chronic neurodegenerative diseases (Alzheimer's disease, Parkinson's disease), "acute" neuronal disorders (stroke, traumatic brain injury, pain signaling), kidney diseases (glomerulonephritis, lupus nephritis, collapsing glomerulopathy, polycystic kidney disease, cisplatin-induced nephrotoxicity), pleural inflammation and arthritis, diabetes type 2, viral infections (HSV, HCMV, HPV, HIV), and unicellular parasites (*Plasmodium*, *Leishmania*, etc.,...).[1] Various CDK inhibitors have already been reported to exhibit antiproliferative activities and are in clinical trials against various cancers (Figure 1).[2] Among them, flavopiridol and (*R*)-roscovitine were the first CDK inhibitors to enter in clinical phase. Second-generation CDK inhibitors such as SNS-032 (former BMS-387032), AG-24322, R547, AT7519, AT7119, AZD5438, and PD-0332991 are in advanced preclinical testing or in clinical trials.[3,4] The discovery of (*R*)-roscovitine has been reported in detail previously.[5] This compound is an orally available 2,6,9-trisubstituted purine that specifically inhibits CDK1, CDK2, CDK3, CDK5, CDK7, and CDK9 in the submicromolar range. Preclinical studies demonstrate that (*R*)-roscovitine acts on multiple phases of the cell cycle and works by inducing cell cycle arrest and apoptosis.[6]

The 2,6,9-trisubstituted purine family **I** (Figure 2) has been the subject of intensive structure−activity relationship studies to identify more potent CDK inhibitory purine derivatives. Thus, the modification of the nature of the substituents on positions 2, 6, and 9 led to the preparation of aminopurvalanol, purvalanol A and B, displaying higher inhibitory CDK activities in vitro.[7] Among the classical approaches to drug design, the bioisosterism strategy[8] is a powerful way to the rational design of new drugs. Several features are favorable to this approach such as (1) improvement of the metabolic stability of the drugs, (2) reduction of certain adverse affects, (3) optimization of pharmacokinetics and/or bioavailability, and (4) circumventing patent issues. In this article, we report a bioisosterism study leading to an original and promising new CDK inhibitor lead compound based on (*R*)-roscovitine.

The pyrazolo[1,5-*a*]-1,3,5-triazine moiety **II** or the imidazo[2,1-*f*]-1,2,4-triazine core **III** allows one to consider the synthesis of a large number of "carbabioisosteres" of purine drugs (Figure 2). In the case of the pyrazolo[1,5-*a*]-1,3,5-triazine moiety, this scaffold perfectly mimicks the biophysicochemical properties of the purine ring[9] while being more stable in vivo (no action of nucleosidases on C-8 position as encountered for the purine ring).[10] By this approach, a large number of pyrazolo[1,5-*a*]-1,3,5-triazine derivatives have been designed for the last several decades as remarkable purine bioisosteres. Thus, this type of modification can lead to a large number of derivatives showing potent biological activities.[11]

These data prompted us to synthesize novel pyrazolo[1,5-*a*]-1,3,5-triazine and imidazo[2,1-*f*]-1,2,4-triazine roscovitine bioisosteres in order to compare their CDK inhibitory and antiproliferative activities to genuine (*R*)-roscovitine.

Results and Discussion

Chemistry. Pyrazolo[1,5-*a*]-1,3,5-triazine derivatives **7a**−**c** were first prepared (Scheme 1). Regioselective iodination on C-8 position of **1**[12] was carried out in the presence of

* To whom correspondence should be addressed. For P.B. (chemistry, chemoinformatic): phone, +33 (0)2 38 25 99 80; fax, +33 (0)2 38 25 99 65; E-mail: philippe.bernard@greenpharma.com. For L.M. (biochemistry and cell biology): phone, +33 (0)2 98 29 23 39; fax, +33 (0)2 98 29 25 26; E-mail: meijer@sb-roscoff.fr. For B.J. (chemistry): phone, +33 (0)4 72 44 81 35; fax, +33 (0)4 72 43 12 14; E-mail: benoit.joseph@univ-lyon1.fr.

[†] Institut de Chimie et Biochimie Moléculaires et Supramoléculaires, UMR-CNRS 5246, Laboratoire de Chimie Organique 1, Université de Lyon, Université Claude Bernard-Lyon 1.

[‡] CNRS, "Protein Phosphorylation & Human Disease" Group, Station Biologique.

[§] Laboratory of Experimental Carcinogenesis, Lombardi Comprehensive Cancer Center, Georgetown University Medical Center.

[||] Aptanomics SA.

[⊥] Greenpharma SA.

10.1021/jm801340z CCC: $40.75
Published on Web 01/07/2009

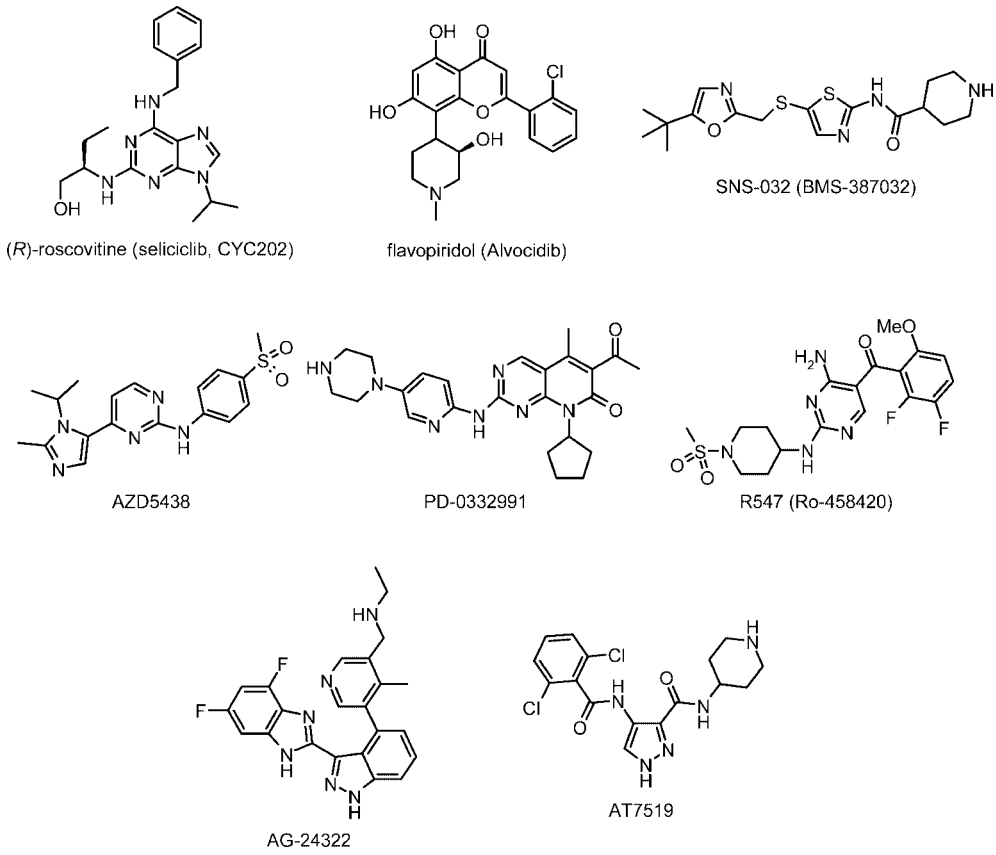

Figure 1. CDK inhibitors in clinical trials: (*R*)-roscovitine, flavopiridol, SNS-032, AZD5438, PD-0332991, R547, AG-24322, and AT7519.

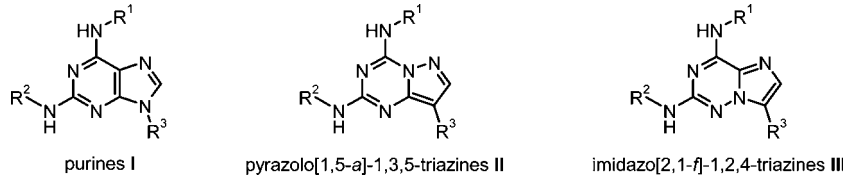

Figure 2. 2,6,9-Trisubstituted purine CDK inhibitor scaffold **I** and related bioisosteres **II** and **III**.

N-iodosuccinimide to give 8-iodopyrazolo[1,5-*a*]-1,3,5-triazine **2**[13] in 88% yield. Introduction of the acetyl group on C-8 position was first performed through a Stille palladium-catalyzed coupling reaction. Derivative **2** was treated with *n*-tributyl(1-ethoxyvinyl)tin in DMF, in the presence of a catalytic amount of freshly prepared *tetrakis*(triphenylphosphine)palladium (8 mol%) and LiCl to provide derivative **3**[13] in good yield. Similarly, compound **3** was prepared from **1** by a Friedel−Crafts acylation.[12] In a sealed tube, compound **1** was submitted to acylation reaction with acetyl chloride in the presence of 1 M $SnCl_4$ in CH_2Cl_2 at 85 °C, affording compound **3** in 86% yield (versus 74% for two steps). The same reaction was carried out under various conditions (AcCl, $AlCl_3$, CH_2Cl_2, room temperature to reflux, or AcCl, $SnCl_4$, CH_2Cl_2, reflux) leading to the total recovery of the starting material. Nucleophilic addition of 1 M MeMgBr in Et_2O on **3** followed by hydrolysis by a freshly prepared NH_4Cl solution gave tertiary alcohol, which was readily treated by sodium borohydride/trifluoroacetic acid in CH_2Cl_2 at room temperature to yield isopropyl derivative **4**. Direct access to **4** from **1** via a Friedel−Crafts alkylation was investigated. Attempts were performed using **1**, isopropyl chloride or iodide and Lewis acids ($AlCl_3$, $SnCl_4$, 1 M $SnCl_4$ in CH_2Cl_2) under different temperature conditions (room temperature to 100 °C in a sealed tube). In each case, the starting material was recovered. As already mentioned in the literature,[10] the *N*-methyl-*N*-phenylamino group on C-4 position is a good leaving group for nucleophilic addition−elimination reaction. Nucleophilic aromatic substitution on C-4 position of **4** was performed either in the presence of benzylamine or 3-chloroaniline, providing secondary amines **5a** and **5b**, respectively, in 84 and 40% yield. *m*-CPBA oxidation of methylsulfanyl group of **5** furnished sulfones **6a** and **6b** in fair yields. (*R*)-roscovitine bioisostere **7a** (N-&-N1, GP0210)[14] was obtained by nucleophilic aromatic substitution on C-2 position of **6a** in the presence of (*R*)-(−)-2-aminobutanol. The enantiomer **7b** was prepared from **6a** and (*S*)-(+)-2-aminobutanol. Purvalanol A bioisostere **7c** was obtained from **6b** and (*R*)-(−)-2-amino-3-methylbutanol.

The synthesis of imidazo[2,1-*f*]-1,2,4-triazine bioisostere was carried out in four steps from the known 6-amino-3,5-bis-(methylsulfanyl)-1,2,4-triazine **8**[15] as depicted in Scheme 2. Treatment of **8** with 2-bromo-3-methylbutyraldehyde dimethyl acetal **9**[16] and molecular sieves 4 Å in the presence of a catalytic amount of camphorsulfonic acid in acetonitrile at reflux led to **10** in 60% yield. Nucleophilic displacement of the methylsulfonyl substitutent on C-4 position of **10** by benzylamine in excess gave compound **11** in good yield. It should be noted that the first experiments were carried out in ethanol at 50 °C, but even after a prolonged reaction time, the reactions were not complete. Optimal condition reaction was finally obtained when benzylamine was used as reagent and solvent. The 2-methyl-

Scheme 1[a]

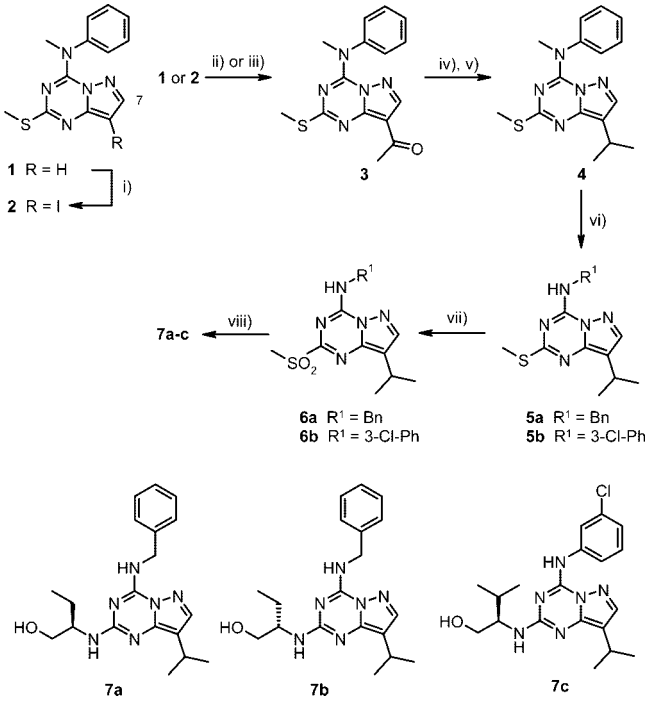

[a] Conditions: (i) NIS, $CHCl_3$, reflux, 90 min, 88%. (ii) AcCl, 1 M $SnCl_4$, CH_2Cl_2, 85 °C, 17 h, sealed tube, 86%. (iii) *n*-Tributyl(1-ethoxyvinyl)stannane, $Pd(PPh_3)_4$, LiCl, DMF, 80−90 °C, 12 h, 84%. (iv) (a) 1 M MeMgBr, THF, 0 °C to rt, 20 min; (b) NH_4Cl. (v) $NaBH_4$, TFA, CH_2Cl_2, 0 °C to rt, 1 h, 89% (two step yield). (vi) Benzylamine, EtOH, 90 °C, 12 h, **5b** = 84%; 3-chloroaniline, dioxane, 120 °C, 12 h, **5a** = 40%. (vii) *m*-CPBA, CH_2Cl_2, 0 °C to rt, 3 h, **6a** = 97%, **6b** = 60%. (viii) (*R*)-(−)-2-aminobutanol, dioxane, 140 °C, 12 h, **7a** = 56%; (*S*)-(+)-2-aminobutanol, dioxane, 140 °C, 12 h, **7b** = 67%, (*R*)-(−)-2-amino-3-methylbutanol, dioxane, 140 °C, 12 h **7c** = 70%.

sulfanyl substituent was oxidized by *m*-CPBA to give the sulfone **12** in 81% yield. The ultimate nucleophilic aromatic substitution on C-2 position of **12** was carried out at 170 °C in the presence of (*R*)-(−)-2-aminobutanol in excess to afford (*R*)-roscovitine analogue **13** (N-&-N2, GP0212)[14] in fair yield.

Biological Evaluation. Inhibition of Cyclin-Dependent Kinases. We first tested the synthesized compounds on a selection of CDKs (CDK1, CDK2, CDK5, CDK7, and CDK9), known to be inhibited by (*R*)-roscovitine.[6] Results show that all compounds were active on these kinases in the submicromolar range (Table 1). Compound **13** was essentially identical to (*R*)-roscovitine in terms of its effects on the 5 CDKs. In contrast, the roscovitine bioisostere **7a** was significantly more potent, by a factor of 3−5, than either **13** or (*R*)-roscovitine. The purvalanol A analogue **7c** was also more potent but, surprisingly, totally inactive on CDK7/cyclin H and CDK9/cyclin T. The enzymatic effects and selectivity of both **7a** and **13** are described in more detail elsewhere.[14]

Inhibition of Tumor Cell Proliferation. We next tested the synthesized compounds for their effects on cell survival using the human neuroblastoma SH-SY5Y and human embryonic kidney HEK293 cell lines (Table 2). Results show that while compound **13** and (*R*)-roscovitine share a similar efficacy, **7a** and its (*S*)-isomer **7b** are significantly more active (5−6 fold). Interestingly, **7c** was completely inactive, possibly accounting for its lack of effects on CDK7 and CDK9. Compound **7a** was next evaluated against the full panel NCI of 60 tumor cell lines (mean graphs data for **7a** and (*R*)-roscovitine, see Supporting Information, Figures S1 and S2).[17] The biological data were compared with those available for (*R*)-roscovitine (Table 3). Results show that compound **7a** is on average more potent at inhibiting cell proliferation than (*R*)-roscovitine (14-fold in terms of GI_{50}, 9-fold in terms of TGI) but only modestly more potent at inducing net cell death (LC_{50}). Nevertheless, the cytotoxic effect of **7a** is preferably observed on melanoma cancer cell lines (see Table 3). Furthermore, like for (*R*)-roscovitine, no specific tumor type displayed any particular sensitivity to compound **7a**. Finally, we performed a cell proliferation assay on a small panel of 6 human cell lines derived from lung (A549), prostate (PC3), cervix (Hela), kidney (293T) cancers, B-lymphoma (Raji), and myeloma (U937) (see Supporting Information, Figure S3). **7a** inhibited the proliferation of all cell lines in a dose-dependent fashion. Total growth inhibition was nearly achieved at 5 μM for the other cell lines. In this assay as well, **7a** proved significantly more potent than (*R*)-roscovitine (Supporting Information, Figure S3), which only partially inhibited tumor cell proliferation at 10 μM. All these data confirm that **7a** is >5-fold more potent than its parent molecule, (*R*)-roscovitine. A more detailed investigation on the intracellular mechanism of action of **7a** and **13**, in comparison with (*R*)-roscovitine, as well as the cocrystal structures of **7a** and (*R*)-roscovitine with CDK2/cyclin A, is presented elsewhere.[14]

In Vivo Antitumor Activity of Compound 7a and (*R*)-Roscovitine. An Ewing's sarcoma xenograft mouse model system established as described in the Experimental Section was used to compare the antitumor activity of **7a** and (*R*)-roscovitine in vivo. This model was selected on the basis of its clear-cut sensitivity to roscovitine.[18] Compound **7a** was evaluated at 25 mg/kg, and (*R*)-roscovitine was tested at 50 mg/kg. Because compound **7a** was roughly 2 times more potent in vitro than (*R*)-roscovitine (average on 5 kinases, Table 1), the dosing for compound **7a** was chosen as half of that of roscovitine, so that both compounds could be compared on the basis of similar activity. Results showed those 8 days after treatment initiation, and both compounds had slowed tumor growth considerably (Figure 3). At 25 mg/kg, compound **7a** was as active as (*R*)-roscovitine used at a concentration 2-fold higher (50 mg/kg). When tumors in control animals reached an average volume about 2000 mm^3, and animals had to be sacrificed to comply with institutional animal care and use guidelines, tumors in drug-treated animals had reached and average volume of only ∼550 mm^3 (a near 73% inhibition of tumor growth). The inhibitory effect of both drugs on tumor growth was also manifested by the fact that tumors in treated animals took an additional period of about 15 days to reach the maximum volume allowed by institutional tumor burden standards (Figure 3).

Conclusion

A rather straightforward bioisostere design approach, applied to the clinical drug (*R*)-roscovitine, has allowed us to generate one analogue that displays unexpected enhanced inhibitory activity toward the CDK targets. This translates into enhanced cell death inducing activity, a favorable property, which was confirmed on more than 60 cell lines, and an improved in vitro biological activity, which was confirmed in a first animal tumor model. Altogether, this work shows that minor modification can lead to better second generation analogues of (*R*)-roscovitine. These findings support further clinical investigation to determine the therapeutic potential of **7a**.

Experimental Section

Chemistry. General Methods. Commercial reagents (Fluka, Aldrich) were used without purification. Solvents were distillated prior to use. (*R*)-Roscovitine was synthesized as

Scheme 2[a]

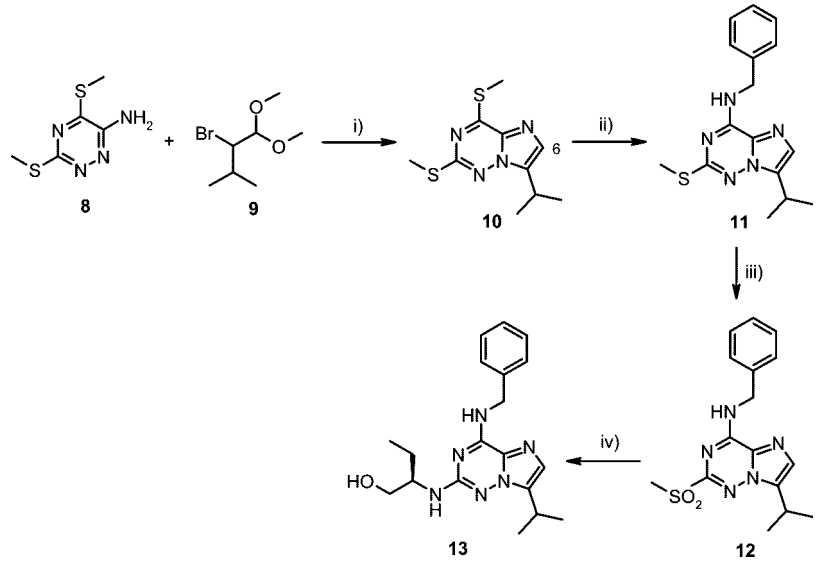

[a] Conditions: (i) CSA, Molecular sieves 4 Å, MeCN, 70 °C, 8 h, 60%; (ii) $BnNH_2$, 50 °C, 16 h, 95%; (iii) *m*-CPBA, CH_2Cl_2, rt, 16 h, 81%; (iv) (*R*)-(−)-2-aminobutanol, 170 °C, 4 h, 60%.

Table 1. Effects of (*R*)-Roscovitine, Purvalanol A, and Its Four Analogues on the Catalytic Activity of Various CDKs[a]

	IC_{50} (μM)[b]				
compd	CDK1/ cyclin B	CDK2/ cyclin A	CDK5/ p25	CDK7/ cyclin H	CDK9/ cyclin T
(*R*)-roscovitine	0.33	0.22	0.27	0.80	0.23
purvalanol A[7a]	0.004	0.070	0.075	ND[c]	ND
7a	0.073	0.04	0.07	0.50	0.043
7b	ND	ND	0.13	ND	ND
7c	0.08	0.06	0.06	>100	>100
13	0.40	0.22	0.32	0.60	0.20

[a] (*R*)-Roscovitine and its analogues were tested at various concentrations for their effects on five CDKs. [b] IC_{50} values were calculated from the dose−response curves and are reported in μM. [c] ND, not determined.

Table 2. Effects of (*R*)-Roscovitine and Its Four Analogues on the Survival of Two Cell Lines[a]

	IC_{50} (μM)[b]	
compd	SH-SY5Y	HEK293
(*R*)-roscovitine	16.1	48.9
7a	2.7	7.6
7b	2.0	7.2
7c	>100	>100
13	15.4	26.8

[a] Compounds were tested at various concentrations for their effects on the survival of the human neuroblastoma SH-SY5Y cells and human embryonic kidney cells (HEK293). [b] Cell survival was estimated 48 h after the addition of each compound using the MTS reduction assay. IC_{50} values were calculated from the dose−response curves and are reported in μM.

described previously[6] and kindly provided by Dr. Hervé Galons and Nassima Oumata (Université René Descartes, Paris 5). Melting points were determined using a Büchi capillary instrument and are uncorrected. IR spectra were recorded on a Perkin-Elmer Spectrum One. ^{1}H spectra were recorded on a Bruker Advance 300 MHz spectrometer. Chemical shifts are reported in ppm (δ) relative to tetramethylsilane as an internal standard. Mass spectra were recorded with a Perkin-Elmer SCIEX API spectrometer. Elemental analyses were performed on a Thermoquest Flash 1112 series EA analyzer. Thin layer chromatography (TLC) analyses were conducted on aluminum sheets silica gel Merck $60F_{254}$. The spots were visualized using an ultraviolet light. Flash chromatography was carried out on silica gel 60 (40 μ63 μM, Merck) using the indicated solvents. The light petroleum ether (PE) refers to the fraction boiling at 40−60 °C.

8-Iodo-4-(*N*-methyl-*N*-phenylamino)-2-(methylsulfanyl)pyrazolo[1,5-*a*]-1,3,5-triazine (2). A solution of 4-(*N*-methyl-*N*-phenylamino)-2-(methylsulfanyl)pyrazolo[1,5-*a*]-1,3,5-triazine **1**[12,13] (940 mg, 3.46 mmol) and NIS (1.09 g, 4.85 mmol) in $CHCl_3$ (35 mL) was stirred at reflux for 30 min. The solvent was evaporated in vacuo. The residue was dissolved in CH_2Cl_2 (50 mL) and washed with a saturated aqueous $Na_2S_2O_3$ solution (3 × 20 mL). The organic layer was dried over $MgSO_4$ and concentrated in vacuo. The crude product was purified by flash chromatography (PE/Et_2O 9:1) to afford **2** (1.21 g, 88%) as a solid; mp 162−163 °C (Et_2O/PE). IR (KBr): ν 3085, 2915, 1605, 1585, 745, 695 cm^{-1}. ^{1}H NMR (300 MHz, $CDCl_3$): δ 7.61 (s, 1H, H_7), 7.39−7.36 (m, 3H, H_{arom}), 7.16 (broad d, 2H, J = 7.1 Hz, H_{arom}), 3.71 (s, 3H, CH_3), 2.59 (s, 3H, CH_3). MS (ESI): *m*/*z* 398 (M + H$^+$). Anal. ($C_{13}H_{12}IN_5S$) C, H, N.

8-Acetyl-4-(*N*-methyl-*N*-phenylamino)-2-(methylsulfanyl)pyrazolo[1,5-*a*]-1,3,5-triazine (3). Method A: A mixture of **1** (871 mg, 3.21 mmol), acetyl chloride (458 mL, 6.42 mmol), and 1 M $SnCl_4$ in CH_2Cl_2 (16.1 mL) was stirred in a sealed tube for 17 h at 85 °C. The reaction mixture was then poured into crushed ice and extracted with EtOAc (3 × 15 mL). The combined organic extracts were dried over $MgSO_4$ and concentrated in vacuo. The crude residue was purified by flash chromatography (CH_2Cl_2/PE/EtOAc 5:6:1) to provide **3** (868 mg, 86%) as a solid. Method B: A mixture of **2** (513 mg, 1.3 mmol), freshly prepared $Pd(PPh_3)_4$ (223 mg, 0.19 mmol), and LiCl (137 mg, 3.23 mmol) in DMF (10 mL) was added to *n*-tributyl(1-ethoxyvinyl)stannane (627 μL, 1.94 mmol). The solution was stirred for 12 h at 90 °C. The solvent was evaporated in vacuo. The crude residue was purified by flash chromatography (CH_2Cl_2/PE/EtOAc 5:6:1) to give **3** (341 mg, 84%) as a solid; mp 223−225 °C (MeOH). IR (KBr): ν 3005, 2935, 1670, 1560, 755, 700 cm^{-1}. ^{1}H NMR (300 MHz, $CDCl_3$): δ 8.08 (s, 1H, H_7), 7.45−7.38 (m, 3H, H_{arom}), 7.19−7.16 (m, 2H, H_{arom}), 3.75 (s, 3H, CH_3), 2.70 (s, 3H, CH_3), 2.59 (s, 3H, CH_3). MS (ESI): *m*/*z* 314 (M + H$^+$). Anal. ($C_{15}H_{15}N_5OS$) C, H, N.

Table 3. Effects of (*R*)-Roscovitine and **7a** on Cell Proliferation and Cell Death as Assayed in the NCI 60 Cell Line Screening Panel[a]

	GI_{50} (μM)[b]		TGI (μM)[c]		LC_{50} (μM)[d]	
cell line	(*R*)-roscovitine	**7a**	(*R*)-roscovitine	**7a**	(*R*)-roscovitine	**7a**
			Leukemia			
CCRF-CEM	>100	0.65	>100	9.26	>100	>100
HL-60(TB)	19.9	0.41	>100	2.68	>100	>100
K-562	50.1	2.44	>100	7.38	>100	>100
MOLT-4	25.1	2.18	>100	9.45	>100	>100
RPMI-8226	25.1	2.23	>100	6.93	>100	>100
SR	5.01	0.25	>100	1.59	>100	>100
			NSCL Cancer			
A549/ATCC	12.6	1.58	>100	41.4	>100	>100
EKVX	19.9	2.41	50.1	9.13	>100	>100
HOP-62	25.1	2.10	>100	8.72	>100	>100
HOP-92	50.1	1.67	>100	7.10	>100	>100
NCI-H226	19.9	1.84	>100	10.1	>100	>100
NCI-H23	12.6	1.71	50.1	7.79	>100	>100
NCI-H322M	31.6	1.86	>100	8.92	>100	>100
NCI-H460	25.1	1.05	>100	10.9	>100	>100
NCI-H522	15.8	1.46	63.1	8.98	>100	>100
			Colon Cancer			
COLO 205	12.6	1.12	31.6	3.15	>100	8.86
HCC-2998	31.6	1.20	>100	3.27	>100	8.96
HCT-116	5.01	0.51	>100	15.0	>100	>100
HCT-15	19.9	0.87	>100	10.5	>100	>100
HT29	19.9	2.00	>100	15.5	>100	>100
KM12	5.01	0.71	63.1	2.79	>100	9.30
SW-620	79.4	1.38	>100	5.56	>100	>100
			CNS Cancer			
SF-268	19.9	1.82	>100	7.20	>100	>100
SF-295	25.1	0.81	>100	4.74	>100	>100
SF-539	15.8	1.22	79.4	3.62	>100	11.9
SNB-19[f]	ND[e]	1.44	ND	12.3	ND	>100
SNB-75	12.6	1.31	31.6	3.33	>100	8.48
U251[f]	50.1	1.40	>100	10.5	>100	>100
			Melanoma			
LOX IMVI	12.6	1.07	>100	10.3	>100	34.4
MALME-3M	19.9	2.60	50.1	6.99	>100	43.5
M14	25.1	2.00	>100	7.93	>100	34.3
SK-MEL-2	15.8	1.47	39.8	6.00	>100	>100
SK-MEL-28	ND	1.16	ND	3.82	ND	16.9
SK-MEL-5	10	1.78	31.6	4.96	79.4	17.4
UACC-257	ND	3.56	ND	15.0	ND	>100
UACC-62	7.9	1.37	31.6	5.50	>100	31.1
			Ovarian Cancer			
IGROV1	6.3	0.78	>100	>100	>100	>100
OVCAR-3	12.6	1.15	>100	4.60	>100	42.4
OVCAR-4	31.6	2.57	>100	37.0	>100	>100
OVCAR-5	39.8	1.85	>100	15.0	>100	>100
OVCAR-8	ND	2.15	ND	54.8	ND	>100
SK-OV-3	79.4	5.55	>100	40.2	>100	>100
			Renal Cancer			
786−0	25.1	1.98	>100	10.7	>100	>100
A498	50.1	1.25	>100	3.44	>100	9.47
ACHN	12.6	0.81	79.4	10.7	>100	49.1
CAKI-1	6.3	1.02	>100	8.35	>100	>100
RXF 393	5.0	0.25	>100	0.79	>100	4.25
SN12C	ND	2.41	ND	14.4	ND	58.1
TK-10	63.1	2.00	>100	10.9	>100	>100
UO-31	12.6	1.59	>100	>100	>100	>100
			Prostate Cancer			
PC-3	19.9	0.93	63.1	12.3	>100	>100
DU-145	15.8	1.30	>100	9.52	>100	>100
			Breast Cancer			
MCF7	12.6	0.59	>100	7.99	>100	>100
NCI/ADR-RES[g]	6.3	2.08	63.1	15.7	>100	>100
MDA-MB-231/ATCC	39.8	2.37	>100	9.47	>100	>100
HS 578T	12.8	1.59	12.6	6.16	79.4	>100
MDA-MB-435[h]	12.6	2.06	50.1	10.1	>100	41.4
BT-549	ND	1.56	ND	5.29	ND	36.1
T-47D	16.8	2.48	79.4	13.3	>100	>100
MDA-MB-468	ND	1.88	ND	5.19	ND	63.5
MG_MID[i]	19.3	1.41	78.3	8.71	99.4	61.6

[a] Data obtained from NCI's in vitro-oriented tumor cells screen ((*R*)-roscovitine = NSC 701554; **7a** = NSC 743927). [b] GI_{50} is the molar concentration causing 50% growth inhibition of tumor cells. [c] TGI is the molar concentration giving total growth inhibition. [d] LC_{50} is the molar concentration leading to 50% net cell death. [e] ND = not determined. [f] CNS cell lines SNB-19 and U251 are derived from the same individual. [g] NCI/ADR-RES is an ovarian tumor cell line, not a breast tumor line. [h] MDA-MB-435 is a melanoma cell line, not a breast cancer cell line cell line. [i] MG_MID (mean graph midpoint) is the arithmetical mean value for all tested cancer lines.

4-(*N*-Methyl-*N*-phenylamino)-8-(1-methylethyl)-2-(methylsulfanyl)pyrazolo[1,5-*a*]-1,3,5-triazine (4). At 0 °C, a solution of 3 M MeMgBr in Et_2O (297 μL, 2.58 mmol) was added dropwise to a solution of **3** (269 mg, 0.86 mmole) in THF (7 mL). After completion of the addition, the solution was stirred at room temperature for an additional 20 min. The reaction

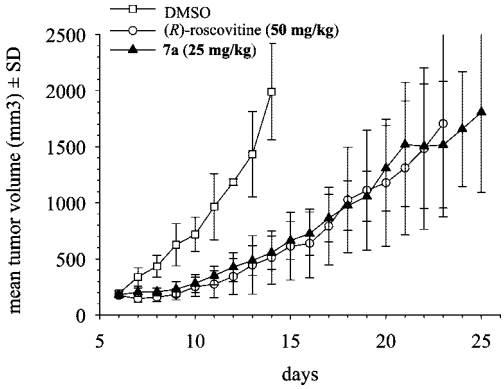

Figure 3. In vivo antitumor activity of **7a**. Compound **7a** treatment of Ewing's sarcoma xenografts established in mice resulted in tumor growth delay similar to that produced by (*R*)-roscovitine. Xenografts established by sc inoculation of A4573 cells (4×10^6 per animal) in nude mice were grown to a mean volume of about 195 mm^3. Animals carrying tumors were randomized into three groups. One group ($n = 6$) was treated with compound **7a** in DMSO, administered as single daily ip injections, at a dose of 25 mg/kg, for five days. Another group ($n = 6$) received (*R*)-roscovitine under the same conditions, except that the dose was 50 mg/kg. The control group ($n = 6$) received ip injections of DMSO following identical schedules. Results shown correspond to one of the experimental replicas. Tumor growths in compound **7a** and (*R*)-roscovitine-treated animals were significantly slower than the growth of tumors in control animals.

mixture was neutralized by a freshly prepared aqueous NH_4Cl solution (5 mL). The aqueous layer was extracted with CH_2Cl_2 (5 mL) and EtOAc (2×5 mL). The combined organic extracts were dried over $MgSO_4$ and concentrated. The oily residue was used without further purification. A solution of the intermediate in CH_2Cl_2 (9 mL) was added at 0 °C under nitrogen atmosphere to a solution of $NaBH_4$ (113 mg, 3.00 mmol) in trifluoroacetic acid (9 mL). The reaction mixture was stirred for 1 h at room temperature and then neutralized by a 1 M NaOH solution (15 mL). The aqueous layer was extracted with CH_2Cl_2 (3×10 mL). The combined organic extracts were dried over $MgSO_4$ and concentrated in vacuo. The residue was purified by flash chromatography (PE/Et_2O 9:1) to afford **4** as a solid (241 mg, 89%); mp 85−87 °C (EtOAc/PE); IR (KBr): ν 3055, 2960, 2865, 1615, 1535, 1460, 750, 695 cm^{-1}. ^1H NMR (300 MHz, $CDCl_3$): δ 7.54 (s, 1H, H_7), 7.41−7.31 (m, 3H, H_{arom}), 7.19−7.15 (m, 2H, H_{arom}), 3.70 (s, 3H, CH_3), 3.14 (hept, 1H, $J = 6.8$ Hz, CH), 2.55 (s, 3H, CH_3), 1.27 (d, 6H, $J = 6.8$ Hz, 2 CH_3). MS (ESI): *m*/*z* 314 ($M + H^+$). Anal. ($C_{16}H_{19}N_5S$) C, H, N.

4-(*N*-Benzylamino)-8-(1-methylethyl)-2-(methylsulfanyl)pyrazolo[1,5-*a*]-1,3,5-triazine (5a). In a sealed tube, a solution of **4** (120 mg, 0.38 mmol) and benzylamine (209 μL, 1.91 mmol) in ethanol (1 mL) was heated for 12 h at 90 °C. Concentration of the reaction mixture provided the crude product that was purified by flash chromatography (PE/Et_2O 4:1) to afford **5a** as a solid (101 mg, 84%); mp 139−141 °C (MeOH). IR (KBr): ν 3280, 2960, 1630, 1605 cm^{-1}. ^1H NMR (300 MHz, $CDCl_3$): δ 7.69 (s, 1H, H_7), 7.33−7.28 (m, 5H, H_{arom}), 6.93 (t, 1H, $J = 6.0$ Hz, NH), 4.78 (d, 2H, $J = 6.0$ Hz, CH_2), 3.15 (hept, 1H, $J = 7.0$ Hz, CH), 2.57 (s, 3H, CH_3), 1.32 (d, 6H, $J = 7.0$ Hz, 2 CH_3). MS (ESI): *m*/*z* 314 ($M + H^+$). Anal. ($C_{16}H_{19}N_5S$) C, H, N.

4-(3-Chloroanilino)-8-(1-methylethyl)-2-(methylsulfanyl)pyrazolo[1,5-*a*]-1,3,5-triazine (5b). In a sealed tube, a solution of **4** (120 mg, 0.38 mmol) and 3-chloroaniline (204 μL, 1.91 mmol) in dioxane (1 mL) was heated for 12 h at 120 °C. After concentration in vacuo, the residue was purified by flash chromatography (PE/Et_2O 20:1 then 9:1) to afford **5b** as a solid (51 mg, 40%); mp 85−87 °C (EtOAc/PE). IR (KBr): ν 3335, 2955, 1615, 1570 cm^{-1}. ^1H NMR (300 MHz, $CDCl_3$): δ 8,.47 (s, 1H, NH), 7.93 (s, 1H, H_{arom}), 7.82 (s, 1H, H_7), 7.60 (d, 1H, $J = 7.5$ Hz, H_{arom}), 7.32 (t, 1H, $J = 8.1$ Hz, H_{arom}), 7.16 (d, 1H, $J = 7.4$ Hz, H_{arom}), 3.19 (hept, 1H, $J = 7.0$ Hz, CH), 2.61 (s, 3H, CH_3), 1.35 (d, 6H, $J = 7.0$ Hz, 2 CH_3). MS (ESI): *m*/*z* 334 ($M + H^+$). Anal. ($C_{15}H_{16}ClN_5S$) C, H, N.

4-(*N*-Benzylamino)-8-(1-methylethyl)-2-(methylsulfonyl)pyrazolo[1,5-*a*]-1,3,5-triazine (6a). Under an inert atmosphere, 50% *m*-CPBA (249 mg, 0.72 mmol) was added to a solution of **5a** (74 mg, 0.24 mmol) in CH_2Cl_2 (5 mL) at 0 °C. The reaction mixture was stirred for 1 h at 0 °C and was allowed to warm up to room temperature for 3 h. The reaction mixture was diluted with CH_2Cl_2 (10 mL), washed with a saturated aqueous $NaHCO_3$ solution (20 mL), and then H_2O (20 mL). The organic phase was dried over $MgSO_4$ and concentrated in vacuo. The crude product was purified by flash chromatography (PE/EtOAc 4:1 then 2:1) to afford **6a** as a solid (81 mg, 97%); mp 123−125 °C (EtOAc/PE). IR (KBr): ν 3395, 2955, 2870, 1645, 1595, 1465, 1045, 750, 700 cm^{-1}. ^1H NMR (300 MHz, $CDCl_3$): δ 7.83 (s, 1H, H_7), 7.43 (t, 1H, $J = 5.9$ Hz, NH), 7.30−7.26 (m, 5H, H_{arom}), 4.82 (d, 2H, $J = 5.9$ Hz, CH_2), 3.29 (s, 3H, CH_3), 3.19 (hept, 1H, $J = 7.0$ Hz, CH), 1.28 (d, 6H, $J = 7.0$ Hz, 2 CH_3). MS (ESI): *m*/*z* 346 ($M + H^+$). Anal. ($C_{16}H_{19}N_5O_2S$) C, H, N.

4-(3-Chloroanilino)-8-(1-methylethyl)-2-(methylsulfonyl)pyrazolo[1,5-*a*]-1,3,5-triazine (6b). Under an inert atmosphere, 50% *m*-CPBA (159 mg, 0.93 mmol) was added to a solution of **5b** (51 mg, 0.15 mmol) in CH_2Cl_2 (3.5 mL) at 0 °C. The reaction mixture was stirred for 1 h at 0 °C and was allowed to warm up to room temperature for 3 h. The reaction mixture was diluted with CH_2Cl_2 (10 mL), washed with a saturated aqueous $NaHCO_3$ solution (10 mL), and then H_2O (10 mL). The organic phase was dried over $MgSO_4$ and concentrated in vacuo. The crude product was purified by flash chromatography (PE/EtOAc 9:1 then 2:1) to afford **6b** as a solid (34 mg, 60%); mp 172−174 °C (EtOAc/PE). IR (KBr): ν 3295, 2960, 2860, 1625, 1570, 1030, 755, 675 cm^{-1}. ^1H NMR (300 MHz, $CDCl_3$): δ 8.71 (s, 1H, NH), 8.02 (s, 1H, H_7), 7.78−7.76 (m, 2H, H_{arom}), 7.35 (t, 1H, $J = 8.3$ Hz, H_{arom}), 7.18 (d, 1H, $J = 8.3$ Hz, H_{arom}), 3.38 (s, 3H, CH_3), 3.29 (hept, 1H, $J = 7.0$ Hz, CH), 1.37 (d, 6H, $J = 7.0$ Hz, 2 CH_3). MS (ESI): *m*/*z* 366 ($M + H^+$). Anal. ($C_{15}H_{16}ClN_5O_2S$) C, H, N.

2-((*R*)-1-Amino-2-butanol)-4-(*N*-benzylamino)-8-(1-methylethyl)pyrazolo[1,5-*a*]-1,3,5-triazine (7a). In a sealed tube, a solution of **6a** (104 mg, 0.30 mmol) and (*R*)-(−)-2-aminobutanol (142 μL, 1.50 mmol) in dry dioxane (1 mL) was heated for 12 h at 140 °C. After evaporation of the solvent, the residue was purified by flash chromatography (PE/EtOAc 2:1) to afford **7a** as a solid (60 mg, 56%); mp 37−39 °C. $[\alpha]_{589}^{25} = +40.6$ (*c* 0.5, CH_2Cl_2). IR (film): ν 3275, 2960, 2875, 1650, 1600, 1560, 1435, 765, 695 cm^{-1}. ^1H NMR (300 MHz, $CDCl_3$): δ 7.56 (s, 1H, H_7), 7.33−7.24 (m, 5H, H_{arom}), 7.10 (s, 1H, NH), 5.23 (s, 1H, OH), 4.73−4.65 (m, 2H, CH_2), 4.00−3.88 (m, 1H, CH), 3.83 (d, 1H, $J = 10.8$ Hz, CH_2O), 3.66 (dd, 1H, $J = 7.3$, 10.8 Hz, CH_2O), 3.02 (hept, 1H, $J = 6.6$ Hz, CH), 1.70−1.52 (m, 2H, CH_2), 1.28 (d, 6H, $J = 6.6$ Hz, 2 CH_3), 1.03 (t, 3H, $J = 7.4$ Hz, CH_3). MS (EI + VE): *m*/*z* 354 (M^+). Anal. ($C_{19}H_{26}N_6O$) C, H, N.

2-((*S*)-1-Amino-2-butanol)-4-(*N*-benzylamino)-8-(1-methylethyl)pyrazolo[1,5-*a*]-1,3,5-triazine (7b). In a sealed tube, a solution of **6a** (84 mg, 0.24 mmol) and (*S*)-(−)-2-aminobutanol (115 μL, 1.22 mmol) in dry dioxane (1 mL) was heated for

12 h at 140 °C. After evaporation of the solvent, the residue was purified by flash chromatography (PE/EtOAc 1:2) to afford **7b** as a solid (58 mg, 67%); mp 37−39 °C. $[\alpha]_{589}^{25} = -40.6$ (*c* 0.5, CH_2Cl_2). Anal. ($C_{19}H_{26}N_6O$) C, H, N.

2-((1*R*)-(1-Methylethyl)-2-hydroxyethylamino)-4-(3-chloroanilino)-8-(1-methylethyl)pyrazolo[1,5-*a*]-1,3,5-triazine (7c). In a sealed tube, a solution of **6b** (34 mg, 0.09 mmol) and (*R*)-(−)-2-amino-3-methylbutanol (47.5 mg, 0.46 mmol) in dry dioxane (1 mL) was heated for 12 h at 140 °C. After evaporation of the solvent, the residue was purified by flash chromatography (PE/EtOAc 4:1) to afford **7c** as a solid (25 mg, 70%); mp 161−163 °C (EtOAc). $[\alpha]_{589}^{25} = +32.5$ (*c* 0.27, CH_2Cl_2). IR (KBr): ν 3360, 3310, 2955, 1635, 1615, 1575, 1420, 1070, 760, 680 cm^{-1}. ^1H NMR (300 MHz, DMSO-d_6 + D_2O, 75 °C): δ 8.05 (s, 1H, H_{arom}), 7.88 (d, 1H, J = 8.0 Hz, H_{arom}), 7.77 (s, 1H, H_7), 7.38 (t, 1H, J = 8.0 Hz, H_{arom}), 7.16 (d, 1H, J = 8.0 Hz, H_{arom}), 3.83 (q, 1H, J = 5.9 Hz, CH), 3.60−3.50 (m, 2H, CH_2O), 2.96 (hept, 1H, J = 7.0 Hz, CH), 1.92−2.02 (m, 1H, CH), 1.27 (d, 6H, J = 7.0 Hz, 2 CH_3), 0.94 (d, 3H, J = 6.8 Hz, CH_3), 0.93 (d, 3H, J = 6.8 Hz, 3 CH_3). MS (ESI): *m*/*z* 389 (M + H^+). Anal. ($C_{19}H_{25}ClN_6O$) C, H, N.

7-(1-Methylethyl)-2,4-bis(methylsulfanyl)imidazo[2,1-*f*]-1,2,4-triazine (10). A solution of triazine **8**[15] (558 mg, 2.96 mmol), camphorsulphonic acid (50 mg, 0.21 mmol), 2-bromo-3-methylbutyraldehyde dimethyl acetal **9**[16] (0.7 mL), and MS 4 Å (50 mg) in dry MeCN (30 mL) were heated at reflux for 48 h. The reaction was completed by addition of **9** (0.5 mL) to the medium at 24 h. The solids were removed by filtration and washed with CH_2Cl_2. After evaporation in vacuo, the residue was taken up in CH_2Cl_2 (40 mL) and washed with saturated aqueous $NaHCO_3$ solution (10 mL), then brine (10 mL). The organic phase was dried over $MgSO_4$ and concentrated in vacuo. The crude product was purified by flash chromatography (PE/EtOAc 95:5) to give **10** (452 mg, 60%) as a solid; mp 85−86 °C. IR (KBr): ν 2960, 1570, 1510, 1435, 1355, 1150 cm^{-1}. ^1H NMR (300 MHz, $CDCl_3$): δ 7.40 (s, 1H, H_6), 3.40 (hept, 1H, J = 7.0 Hz, CH), 2.66 (s, 3H, CH_3), 2.60 (s, 3H, CH_3), 1.39 (d, 6H, J = 7.0 Hz, 2 CH_3). MS (ESI): *m*/*z* 255 (M + H^+). Anal. ($C_{10}H_{14}N_4S_2$) C, H, N.

4-Benzylamino-7-(1-methylethyl)-2-(methylsulfanyl)imidazo[2,1-*f*]-1,2,4-triazine (11). A mixture of **10** (228 mg, 0.90 mmol) and benzylamine (1 mL) was stirred at 50 °C for 4 h. Amine in excess was removed at 10^{-2} mm Hg using Kugelrohr apparatus. The solid residue was recrystallized from EtOH to yield **11** (232 mg, 83%). Mother liquors were concentrated and the crude residue was purified by flash chromatography (PE/EtOAc 7:3) gel to give an additional quantity (35 mg) of **11** (overall yield: 95%); mp 161−162 °C (EtOH). IR (KBr): ν 3245, 2960, 1620, 1340, 1270, 1195 cm^{-1}. ^1H NMR (300 MHz, $CDCl_3$): δ 7.30−7.34 (m, 5H, H_{arom}), 7.13 (s, 1H, H_6), 6.94 (broad s, 1H, NH), 4.79 (d, 2H, J = 5.6 Hz, CH_2), 3.35 (hept, 1H, J = 7.0 Hz, CH), 2.55 (s, 3H, CH_3), 1.37 (d, 6H, J = 7.0 Hz, 2 CH_3). MS (ESI): *m*/*z* 314 (M + H^+). Anal. ($C_{16}H_{19}N_5S$) C, H, N.

4-Benzylamino-7-(1-methylethyl)-2-(methylsulfonyl)imidazo[2,1-*f*]-1,2,4-triazine (12). To an ice-cold solution of **11** (331 mg, 1.06 mmol) in CH_2Cl_2 (10 mL) was added 70% *m*-CPBA (781 mg, 3.17 mmol) in small portions. The reaction was stirred for 30 min at 0 °C then 3.5 h at room temperature. The mixture was diluted in CH_2Cl_2 (10 mL), washed with saturated aqueous $NaHCO_3$ solution (10 mL), and then brine (10 mL). The organic phase was dried over $MgSO_4$ and concentrated in vacuo. The crude residue was purified by flash chromatography (PE/EtOAc 85:15 to 1:1) to provide **12** (295 mg, 81%) as a solid; mp 132−133 °C (EtOH). IR (KBr): ν 3250, 2970, 1620, 1380, 1330, 1145, 970, 755 cm^{-1}. ^1H NMR (300 MHz, $CDCl_3$): δ 7.40 (broad s, 1H, NH), 7.31−7.39 (m, 6H, H_{arom} + H_6), 4.88 (d, 2H, J = 5.8 Hz, CH_2), 3.43 (hept, 1H, J = 7.0 Hz, CH), 3.32 (s, 3H, CH_3), 1.39 (d, 6H, J = 7.0 Hz, 2 CH_3). MS (ESI): *m*/*z* 346 (M + H^+). Anal. ($C_{16}H_{19}N_5O_2S_2$) C, H, N.

2-((*R*)-1-Amino-2-butanol)-4-(*N*-benzylamino)-7-(1-methylethyl)imidazo[2,1-*f*]-1,2,4-triazine (13). A mixture of **12** (253 mg, 0.73 mmol) and (*R*)-(−)-2-aminobutanol (0.35 mL, 3.7 mmol) was heated for 4 h at 170 °C. Excess of amine was removed by Kugelrohr distillation at 10^{-2} mmHg, and the crude residue was purified by flash chromatography (PE/EtOAc 6:4 to 1:1) to give **13** (155 mg, 60%) as a solid; mp 105−106 °C (PE/EtOAc 8:2). $[\alpha]_{589}^{25} = +50.8$ (*c* 0.5, $CHCl_3$). IR (KBr): ν 3330, 3220, 3100, 1615, 1570, 1540, 1450, 1370, 1055, 755, 720 cm^{-1}. ^1H NMR (300 MHz, $CDCl_3$): δ 7.34−7.27 (m, 5H, H_{arom}), 7.08 (s, 1H, H_6), 6.89 (broad s, 1H, NH), 4.73 (d, 2H, J = 5.5 Hz, CH_2), 4.57 (d, 1H, J = 6.4 Hz, OH), 3.89−3.78 (m, 2H, CH_2O + CH), 3.70−3.60 (m, 1H, CH_2O), 3.37 (broad s, 1H, NH), 3.24 (hept, 1H, J = 7.0 Hz, CH), 1.73−1.51 (m, 2H, CH_2), 1.35 (d, 3H, J = 7.0 Hz, CH_3), 1.34 (d, 3H, J = 7.0 Hz, CH_3), 1.02 (t, 1H, J = 7.4 Hz, CH_3). MS (EI + VE): *m*/*z* 354 (M^+). Anal. ($C_{19}H_{26}N_6O$) C, H, N.

Biology. Protein Kinase Assays. CDK1/cyclin B (native affinity purified from starfish oocytes), CDK2/cyclin A, CDK7/cyclin H, CDK9/cyclin T (human recombinant, expressed in baculovirus-infected insect cells), and CDK5/p25 (human recombinant, expressed in *E. coli*) were assayed in the presence of 15 μM ATP as previously described.[16] IC_{50} values were determined from dose−response curves and are expressed in μM.

Cell Cultures and Reagents. A549, PC3, Hela, and 293T cells were cultured in complete medium (DMEM without phenol red, supplemented with 10% heat-inactivated fetal calf serum, 2 mM Glutamax-I, 100 IU/mL penicillin, 100 μg/mL streptomycin). Raji and U937 cells were cultured in complete medium (RPMI 1640 without phenol red supplemented with 10% heat-inactivated fetal calf serum, 2 mM Glutamax-I, 100 IU/mL penicillin, 100 μg/mL streptomycin). All cells were kept at 37 °C in a humidified atmosphere (5% CO_2 in air). Exponentially growing cells were used for all experiments. Cell culture reagents were purchased from Invitrogen. SH-SY5Y human neuroblastoma cell line was grown in DMEM supplemented with 2 mM L-glutamine (Invitrogen, Cergy Pontoise, France) plus antibiotics and a 10% volume of FCS (Invitrogen). Cell viability was determined by means of the MTS (3-(4,5-dimethylthiazol-2-yl)-5-(3-carboxymethoxyphenyl)-2-(4-sulfophenyl)-2*H*-tetrazolium) method as previously described in detail.[19] Roscovitine was purchased from Sigma-Aldrich and dissolved in DMSO to make a 10 mM stock, which was then diluted as desired into complete medium. The DMSO concentration was kept equal to 0.1% in all cell culture wells.

Cell Proliferation Assays. Five thousand cells of each cell line were seeded in 90 μL of culture medium/well in 96-well plates (Greiner, no. 655098), and we incubated the plates for 6 h at 37 °C. We then added different concentrations of (*R*)-roscovitine or compound **7a** in triplicate, and plates were incubated for 72 h. To quantify viable cells at the beginning of the experiment, a Vialight assay (Cambrex, no. LT07−121) was used in a control plate where cells were treated with 0.1% DMSO. Briefly, 50 μL of cell lysis buffer were added, followed by a 10 min incubation at room temperature. Then 100 μL of Vialight assay buffer was added, and after a 2 min incubation, luminescence was recorded in each well with an Envision plate

reader (Perkin-Elmer). The average luminescence value was calculated on 6 wells for each cell line. After 72 h, a Vialight assay was performed on all test plates and on the control plate.

In Vivo Antitumor Activity. Experiments to evaluate the antitumor activity of compound **7a** were carried out essentially as previously described[14,19] under protocols approved by the Georgetown University Animal Care and Use Committee, using immunodeficient, male (5−6 weeks old) athymic nude (BALB/c *nu*/*nu*) mice purchased from the National Cancer Institute.[20] Mice were injected sc into the right posterior flank with 4×10^6 A4573 Ewing's sarcoma cells in 100 μL of Matrigel basement membrane matrix (BD Biosciences, San Jose, California). Once tumors reached a mean volume of about 195 mm^3, mice were randomized into three groups (six animals per group) and treatment was initiated. Experimental groups were treated with compound **7a** or (*R*)-roscovitine, dissolved in DMSO, and administered as a single daily ip injection, at a dose of 25 or 50 mg/kg, respectively, for 5 days. The control group received ip injections of DMSO following an identical schedule. Tumor growth was followed for up to 4 weeks after the first injection. Tumor volumes were calculated by the formula $V = (1/2)a \times b^2$, where a is the longest tumor axis, and b is the shortest tumor axis. Whenever tumors reached the maximum volume allowed by institutional tumor burden guidelines, animals were sacrificed by asphyxiation with CO_2. Tumors were immediately excised from euthanized animals and measured. Data are given as mean values ± SD. Statistical analysis of differences between groups was performed by a one-way ANOVA, followed by an unpaired Student's *t* test.

Acknowledgment. This research was supported by grants from the EEC (FP6-2002-Life Sciences & Health, PRO-KINASE Research Project) (L.M.), the "Cancéropole Grand-Ouest" grant (L.M.), from the "Institut National du Cancer" (INCa), Cancer Détection d'Innovations 2006 (L.M.), from the "Ligue Nationale contre le Cancer" (L.M.), and by U.S. NIH grant PO1-CA74175 (V.N.). K.B. was supported by a fellowship from the "Ministère de la Recherche" and from the "Association pour la Recherche sur le Cancer". We are grateful to J. Boix for the SH-SY5Y cell line. We thank the National Cancer Institute (Bethesda, MD) for the antitumor tests reported in this paper.

Supporting Information Available: Elemental analyses; NCI 60 mean graphs data for **7a**; NCI 60 mean graphs data for (*R*)-roscovitine; the effects of (*R*)-roscovitine (**A**) and **7a** (**B**) on growth of six human tumor cell lines (A549, PC3, Hela, 293T, Raji, and U937). This material is available free of charge via the Internet at http://pubs.acs.org.

References

(1) (a) Shapiro, G. I. Cyclin-dependent kinase pathways as targets for cancer treatment. *J. Clin. Oncol.* **2006**, *24*, 1770–1783. (b) Du, J.; Widlund, H. R.; Horstmann, M. A.; Ramaswamy, S.; Ross, K.; Huber, W. E.; Nishimura, E. K.; Golub, T. R.; Fisher, D. E. Critical role of CDK2 for melanoma growth linked to its melanocyte-specific transcriptional regulation by MITF. *Cancer Cell* **2004**, *6*, 565–576. (c) Alvi, A. J.; Austen, B.; Weston, V. J.; Fegan, C.; MacCallum, D.; Gianella-Borradori, A.; Lane, D. P.; Hubank, M.; Powell, J. E.; Wei, W.; Taylor, A. M. R.; Moss, P. A. H.; Stankovic, T. A novel CDK inhibitor, CYC202 (R-roscovitine), overcomes the defect in p53-dependent apoptosis in B-CLL by down-regulation of genes involved in transcription regulation and survival. *Blood* **2005**, *105*, 4484–4491. (d) Cruz, J. C.; Tsai, L. H. Cdk5 deregulation in the pathogenesis of Alzheimer's disease. *Trends Mol. Med.* **2004**, *10*, 452–458. (e) Smith, P. D.; O'Hare, M. J.; Park, D. S. CDKs: taking on a role as mediators of dopaminergic loss in Parkinson's disease. *Trends Mol. Med.* **2004**, *10*, 445–451. (f) Zhang, M.; Li, J.; Chakrabarty, P.; Bu, B.; Vincent, I. Cyclin-dependent kinase inhibitors attenuate protein hyper-phosphorylation, cytoskeletal lesion formation, and motor defects in Niemann−Pick Type C mice. *Am. J. Pathol.* **2004**, *165*, 843–853. (g) Wang, J.; Liu, S.; Fu, Y.; Wang, J. H.; Lu, Y. Cdk5 activation induces hippocampal CA1 cell death by directly phosphorylating NMDA receptors. *Nat. Neurosci.* **2003**, *6*, 1039–1047. (h) Di Giovanni, S.; Movsesyan, V.; Ahmed, F.; Cernak, I.; Schinelli, S.; Stoica, B.; Faden, A. I. Cell cycle inhibition provides neuroprotection and reduces glial proliferation and scar formation after traumatic brain injury. *Proc. Natl. Acad. Sci. U.S.A.* **2005**, *102*, 8333–8338. (i) Pareek, T. K.; Keller, J.; Kesavapany, S.; Pant, H. C.; Iadarola, M. J.; Brady, R. O.; Kulkani, A. B. Cyclin-dependent kinase 5 activity regulates pain signaling. *Proc. Natl. Acad. Sci. U.S.A.* **2006**, *103*, 791–796. (j) Pareek, T. K.; Keller, J.; Kesavapany, S.; Agarwal, N.; Kuner, R.; Pant, H. C.; Iadarola, M. J.; Brady, R. O.; Kulkarni, A. B. Cyclin-dependent kinase 5 modulates nociceptive signaling through direct phosphorylation of transient receptor potential vanilloid 1. *Proc. Natl. Acad. Sci. U.S.A.* **2007**, *104*, 660–665. (k) Gherardi, D.; D'Agati, V.; Chu, T.-H. T.; Barnett, A.; Gianella-Borradori, A.; Gelman, I. H.; Nelson, P. J. Reversal of collapsing glomerulopathy in mice with the cyclin-dependent kinase inhibitor CYC202. *J. Am. Soc. Nephrol.* **2004**, *15*, 1212–1222. (l) Griffin, S. V.; Krofft, R. D.; Pippin, J. W.; Shankland, S. J. Limitation of podocyte proliferation improves renal function in experimental crescentic glomerulonephritis. *Kidney Int.* **2005**, *67*, 977–986. (m) Bukanov, N. O.; Smith, L. A.; Klinger, K. W.; Ledbetter, S. R.; Ibraghimov-Beskrovnaya, O. Long-lasting arrest of murine polycystic kidney disease with CDK inhibitor Roscovitine. *Nature* **2006**, *444*, 949–952. (n) Price, P. M.; Yu, F.; Kaldis, P.; Aleem, E.; Nowak, G.; Safirstein, R. L.; Megyesi, J. Dependence of cisplatin-induced cell death in vitro and in vivo on cyclin-dependent kinase 2. *J. Am. Soc. Nephrol.* **2006**, *17*, 2434–2442. (o) Rossi, A. G.; Sawatzky, D. A.; Walker, A.; Ward, C.; Sheldrake, T. A.; Riley, N. A.; Caldicott, A.; Martinez-Losa, M.; Walker, T. R.; Duffin, R.; Gray, M.; Crescenzi, E.; Martin, M. C.; Brady, H. J.; Savill, J. S.; Dransfield, I.; Haslett, C. Cyclin-dependent kinase inhibitors enhance the resolution of inflammation by promoting inflammatory cell apoptosis. *Nat. Med.* **2006**, *12*, 1056–1064. (p) Wei, F.-Y.; Nagashima, K.; Ohshima, T.; Saheki, Y.; Lu, Y.-F.; Matsushita, M.; Yamada, Y.; Mikoshiba, K.; Seino, Y.; Matsui, H.; Tomizawa, K. Cdk5-dependent regulation of glucose-stimulated insulin secretion. *Nat. Med.* **2005**, *11*, 1104–1108. (q) Kitani, K.; Oguma, S.; Nishiki, T. I.; Ohmori, I.; Galons, H.; Matsui, H.; Meijer, L.; Tomizawa, K. A Cdk5 inhibitor enhances the induction of insulin secretion by exendin-4 both in vitro and in vivo. *J. Physiol. Sci.* **2007**, *57*, 235–239. (r) Pumfery, A.; De La Fuente, C.; Berro, R.; Nekhai, S.; Kashanchi, F.; Chao, S.-H. Potential use of pharmacological cyclin-dependent kinase inhibitors as anti-HIV therapeutics. *Curr. Pharm. Des.* **2006**, *12*, 1949–1961. (s) Doerig, C.; Billker, O.; Pratt, D.; Endicott, J. Protein kinases as targets for antimalarial intervention: Kinomics, structure-based design, transmission-blockade, and targeting host cell enzymes. *Biochim. Biophys. Acta* **2005**, *1754*, 132–150.

(2) Knockaert, M.; Greengard, P.; Meijer, L. Pharmacological inhibitors of cyclin-dependent kinases. *Trends Pharmacol. Sci.* **2002**, *123*, 417–425.

(3) Sharma Sapra, P.; Sharma, R.; Tyagi, R. Inhibitors of cyclin dependent kinases: useful targets for cancer treatment. *Curr. Cancer Drug Targets* **2008**, *8*, 53–75.

(4) Malumbres, M.; Pevarello, P.; Barbacid, M.; Bischoff, J. R. CDK inhibitors in cancer therapy: what is next? *Trends Pharmacol. Sci.* **2008**, *29*, 16–21.

(5) Meijer, L.; Raymond, E. Roscovitine and other purines as kinase inhibitors. From starfish oocytes to clinical trials. *Acc. Chem. Res.* **2003**, *36*, 417–425.

(6) Meijer; L.; Bettayeb, K.; Galons, H. (*R*)-Roscovitine (CYC202, Seliciclib). In *Inhibitors of Cyclin-Dependent Kinases as Anti-tumor Agents*; Enzyme Inhibitors Series, Volume 3Smith, P. J., Yue, E. W., Eds.; CRC Press: Boca Raton, FL, 2006; Chapter 9, pp 187−226.

(7) (a) Gray, N. S.; Wodicka, L.; Thunnissen, A.-M. W. H.; Norman, T. C.; Kwon, S.; Espinoza, F. H.; Morgan, D. O.; Barnes, G.; LeClerc, S.; Meijer, L.; Kim, S.-H.; Lockhart, D. J.; Schultz, P. G. Exploiting chemical libraries, structure, and genomics in the search for kinase inhibitors. *Science* **1998**, *281*, 533–538. (b) Chang, Y.-T.; Gray, N. S.; Rosania, G. R.; Sutherlin, D. P.; Kwon, S.; Norman, T. C.; Sarohia, R.; Leost, M.; Meijer, L.; Schultz, P. G. Synthesis and application of functionally diverse 2,6,9-trisubstituted purine libraries as CDK inhibitors. *Chem. Biol.* **1999**, *6*, 361–375.

(8) (a) Patani, G. A.; LaVoie, E. J. Bioisosterism: a rational approach in drug design. *Chem. Rev.* **1996**, *96*, 3147–3176. (b) Moreira Lima, L.; Barreiro, E. J. Bioisosterism: a useful strategy for molecular modification and drug design. *Curr. Med. Chem.* **2005**, *12*, 23–49.

(9) Raboisson, P.; Schultz, D.; Muller, C.; Reimund, J.-M.; Pinna, G.; Mathieu, R.; Bernard, P.; Do, Q.-T.; DesJarlais, R. L.; Justiano, H.; Lugnier, C.; Bourguignon, J.-J. Cyclic nucleotide phosphodiesterase type 4 inhibitors: evaluation of pyrazolo[1,5-*a*]-1,3,5-triazine ring

system as an adenine bioisostere. *Eur. J. Med. Chem.* **2008**, *43*, 816–829.
(10) Raboisson, P.; Baurand, A.; Cazenave, J.-P.; Gachet, C.; Schultz, D.; Spiess, B.; Bourguignon, J.-J. General approach toward the synthesis of C-nucleoside pyrazolo[1,5-*a*]-1,3,5-triazines and their 3′,5′-bisphosphate C-nucleotide analogues as the first reported in vivo stable $P2Y_1$-receptor antagonists. *J. Org. Chem.* **2002**, *67*, 8063–8071.
(11) Dolzhenko, A. V.; Dolzhenko, A. V.; Chui, W.-K. Pyrazolo[1,5-*a*][1,3,5]triazines (5-aza-9-deazapurines): synthesis and biological activity. *Heterocycles* **2008**, *75*, 1575–1622.
(12) Raboisson, P.; Schultz, D.; Lugnier, C.; Bourguignon, J. J. Efficient synthesis of 8-substituted pyrazolo[1,5-*a*]-1,3,5-triazines by regioselective acylation. *Tetrahedron Lett.* **2002**, *43*, 9501–9503.
(13) Popowycz, F.; Bernard, P.; Raboisson, P.; Joseph, B. Synthesis of 8-substituted pyrazolo[1,5-*a*]-1,3,5-triazine derivatives via palladium-catalyzed cross-coupling reactions. *Synthesis* **2007**, 367–374.
(14) Bettayeb, K.; Sallam, H.; Ferandin, Y.; Popowycz, F.; Fournet, G.; Hassan, M.; Echalier, A.; Bernard, P.; Endicott, J.; Joseph, B.; Meijer, L. N-&-N, a new class of cell death-inducing, kinase inhibitors derived from the purine roscovitine. *Mol. Cancer Ther.* **2008**, *7*, 2713–2724.
(15) (a) Dudfield, P. J.; Le, V.-D.; Lindell, S. D.; Rees, C. W. Synthesis of C-ribosyl imidazo[2,1-*f*][1,2,4]triazines as inhibitors of adenosine and AMP deaminases. *J. Chem. Soc., Perkin Trans. 1* **1999**, *20*, 2929–2936. (b) Tzeng, C. C.; Motola, N. C.; Panzica, R. P. Synthesis of certain 5,6-diamino-as-triazines: precursors for fused heterocyclic systems. *J. Org. Chem.* **1983**, *48*, 1271–1275.
(16) Rasmussen, P. B.; Boewadt, S. Ketene chemistry. 2. A general procedure for the synthesis of 2-alkoxycyclopropanecarboxylic esters and acids starting from aldehydes and ketene. *Synthesis* **1989**, 114–117.
(17) (a) Paull, K. D.; Hamel, E.; Malspeis, L., Prediction of biochemical mechanism of action from the in vitro antitumor screen of the National Cancer Institute. In *Cancer Chemotherapeutic Agents*; Foye, W. O., Ed.; American Chemical Society: Washington, DC, 1995; Chapter 2, pp 9−45. Also available online at http://dtp.nci.nih.gov/docs/compare/compare.html. (b) Holbeck, S. L. Update on NCI in vitro drug screen utilities. *Eur. J. Cancer* **2004**, *40*, 785–793.
(18) Tirado, O. M.; Mateo-Lozano, S.; Notario, V. Roscovitine is an effective inducer of apoptosis of Ewing's sarcoma family tumor cells in vitro and in vivo. *Cancer Res.* **2005**, *65*, 9320–9327.
(19) Ribas, J.; Boix, J. Cell differentiation, caspase inhibition, and macromolecular synthesis blockage, but not BCL-2 or BCL-XL proteins, protect SH-SY5Y cells from apoptosis triggered by two CDK inhibitory drugs. *Exp. Cell Res.* **2004**, *295*, 9–24.
(20) Developmental Therapeutics Program NCI/NIH, http://dtp.cancer.gov/. Accessed October 2007.

JM801340Z